Evolving three-dimensional cellular automata to perform a quasiperiod-3 collective behavior task

Francisco Jiménez-Morales
Departamento de Física de la Materia Condensada, Universidad de Sevilla, P. O. Box 1065, 41080-Sevilla, Spain
(Received 18 May 1999)

We present results from experiments in which a genetic algorithm (GA) is used to develop three-dimensional cellular automata (CA) to perform a nontrivial collective behavior task. Under a fitness function that is defined as an averaged area in the iterative map, the GA detects a CA rule with quasiperiod-3 (QP3) collective behavior and another with period-3. For rules with QP3 the time autocorrelation function decays as a power law with an exponent of $-1/2$, according to the predictions of the Kardar-Parisi-Zhang equation, and a space-time diagram reveals the existence of propagating structures inside the system. [S1063-651X(99)14910-9]

PACS number(s): 02.70.−c, 82.20.Wt

I. INTRODUCTION

In many natural systems, simple, locally interacting components give rise to coordinated global information processing. In both natural and human-constructed information-processing systems, allowing global coordination to emerge from a decentralized collection of simple components has important potential advantages—e.g., speed, robustness, and evolvability—as compared to explicit central control. However, it is difficult to design a collection of individual components and their interaction in a way that will give rise to useful global information processing or ''emergent computation.'' The term emergent computation refers to the appearance in a system's temporal behavior of information-processing capabilities that are not explicitly represented in the system's elementary components.

In order to understand the mechanisms by which an evolutionary process can detect methods of emergent computation, a simplified framework was proposed and studied by Crutchfield, Mitchell, and co-workers [1–4] in which a genetic algorithm (GA) evolved one-dimensional cellular automata (CAs) to perform computations. In their work, the GA was able to detect CAs with high performance on tasks requiring cooperative collective behavior. The density classification task and the synchronization task are two examples of emergent computation for small radius binary CA. A successful CA for the classification task will determine whether or not the initial configuration contains more than half ones. If it does, the whole lattice should eventually iterate to the fixed-point configuration of all cells in state 1; otherwise, it should eventually iterate to the fixed-point configuration of all zeros. For the synchronization task a successful CA will reach a final configuration in which all cells oscillate between all zeros and all ones on successive time steps.

A much more complex situation of emergent behavior in CAs is found in $d=3$ with the appearance of nontrivial collective behavior (NTCB). Since CAs are governed by local interactions and subjected to noise, it was expected that any global observable would show a trivial time dependence in the limit of infinite size [5]. But several exceptions to this have been found. The most remarkable one is quasiperiod-3 behavior (QP3) that exhibits the concentration of the rule-33 automaton in $d=3$ [6] and other CAs in high space dimensions [7]. This behavior is neither transient nor due to the finite size of the lattice and has been obtained for deterministic and probabilistic rules [8]. At the moment there is no answer to the question of how NTCB can be predicted from the local rule, nor to how we can design a CA with a specific behavior.

In this paper we couple an evolutionary process—a GA—to a population of three-dimensional CAs. The survival of an individual CA is determined by its ability to perform a ''QP3 (P3) task.''

II. CELLULAR AUTOMATA

Cellular automata are regular lattices of variables, each of which can take a finite number of values (''states'') and each of which evolves in discrete time steps according to a local rule that may be deterministic or probabilistic. Physical, chemical, and biological systems with many discrete elements with local interactions can be modeled using CAs. The CAs studied here are three dimensional with two possible states per cell (0 or 1) and with periodic boundary conditions. We denote the lattice size (i.e., number of cells) as $N=L^3$. A CA has a single fixed rule ϕ used to update each cell; the rule maps from the states in a neighborhood of cells to a single state $s_{i,j,k}(t)$, which is the updated value for the cell at sites i,j,k in the neighborhood. The lattice starts out with an initial configuration of states and this configuration changes in discrete time steps. The neighborhood of a cell at positions i,j,k consists of the nearest neighbors in $d=3$ (the Von Neumann neighborhood), and it can be displayed (Table I) as a string of seven bits. Note that the number of different neighborhood configurations is $2^7=128$.

The transition rule ϕ can be expressed as a lookup table (a ''rule table''), which lists for each local neighborhood the

TABLE I. A bit string representing the neighborhood of a cell $s_{i,j,k}$.

$s_{i,j,k}$	$s_{i-1,j,k}$	$s_{i+1,j,k}$	$s_{i,j-1,k}$	$s_{i,j+1,k}$	$s_{i,j,k-1}$	$s_{i,j,k+1}$

updated state of the neighborhood's cell at positions i,j,k. A rule is a bit string that consists of 128 bits, and then the range of rules under investigation is of 2^{128}, which is too large for a sequential search.

III. THE QP3 (P3) TASK

The global behavior of the CA is monitored through the concentration of activated cells at time t, $c(t)=(1/n)\Sigma_{i,j,k}^{n} s_{i,j,k}(t)$. According to the time series of the concentration, the types of nontrivial collective behavior reported are noisy period-1 (P1), period-2 (P2), intermittent period-2 (P2i), period-3 (P3), and quasiperiod-3 (QP3). These behaviors are represented by distinct clouds of points in the iterative map, i.e., the plot of $c(t+1)$ versus $c(t)$. P1, P2, and P3 correspond respectively to one, two, and three clouds of points in the iterative map; P2i is period-2 behavior with a nonconstant amplitude of the oscillation $|c(t+1)-c(t)|$; in the iterative map it can be distinguished by one cloud of points along a straight line. Finally, QP3 behavior corresponds to a triangular object. The NTCBs are chaotic in the sense of Wolfram's class III; each site of the lattice follows a chaotic evolution which has no apparent relation to the global one. The global variable $c(t)$ shows fluctuations that decrease as the lattice size increases, leading to a well defined thermodynamic limit. The most interesting NTCBs are P3 and QP3.

The goal in the ''QP3 (P3) task'' is to find a CA that, starting from a random initial configuration, reaches a final configuration in which the concentration oscillates among three different values, i.e., follows P3 or QP3 collective behavior.

The QP3 (P3) task counts as a nontrivial computation for small-radius CA because the CAs depends on computations for which memory requirements increases with L and in which information must be transmitted over significant space-time distances.

IV. DETAILS OF THE EXPERIMENTS

We used a genetic algorithm to evolve three-dimensional, binary state CAs to perform a QP3 (P3) task. GAs are search methods inspired by biological evolution. In a typical GA, candidate solutions to a given problem are encoded as bit strings (''chromosomes''). A population of such strings is chosen at random and evolves over several generations under selection, crossover, and mutation. At each generation, the fitness of each bit string is calculated according to some externally imposed fitness function, and the highest-fitness bit strings are selected preferentially to be the ''parents'' who form a new population via crossover and mutation. Under crossover, pairs of parents exchange bits to form offspring, which are then subject to a small probability of mutation at each bit position. After several generations, the population often contains high-fitness bit strings representing high-quality solutions to the given problem. The search mechanism of a GA requires balancing two objectives: exploiting the best solution and exploring the search space.

The GA that we used begins with a population of P randomly generated chromosomes listing the rule-table output bits in lexicographic order of neighborhood patterns. The

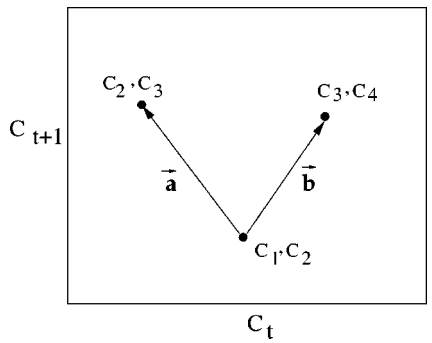

FIG. 1. The iterative map plots the concentration in time $t+1$ versus the concentration in time t. We construct vector $\mathbf{a}=(c_2-c_1,c_3-c_2)$ and vector $\mathbf{b}=(c_3-c_1,c_4-c_2)$. The fitness function $F(\phi)$ is defined as an average of the area in the iterative map, $F=(4/M)\Sigma_i^{M/4}\frac{1}{2}|\mathbf{a}\times\mathbf{b}|_i$.

fitness evaluation for each CA rule is carried out on a lattice of 10^3 cells starting from a random initial condition of concentration 0.5. After a transient time of $N/2$ we allow each rule to run for a maximum number of M iterations. The values of concentration are assembled in groups of four consecutive values and the fitness function $F(\phi)$ is defined by

$$F(\phi)=\frac{4}{M}\sum_{i}^{M/4}\frac{1}{2}\mathrm{abs}[(c_2-c_1)(c_4-c_2)-(c_3-c_2)(c_3-c_1)]_i .$$

We have studied other fitness functions, such as the Shannon information function $S=-K\Sigma_i^n f_i\log(f_i)$ and a function of the range of concentration values, but the best results are obtained with $F(\phi)$. The rule's fitness $F(\phi)$ is taken from a geometrical point of view and it is an average area in the iterative map; see Fig. 1 for more details. In the iterative map the area of a P2 behavior is very-small almost 0; the

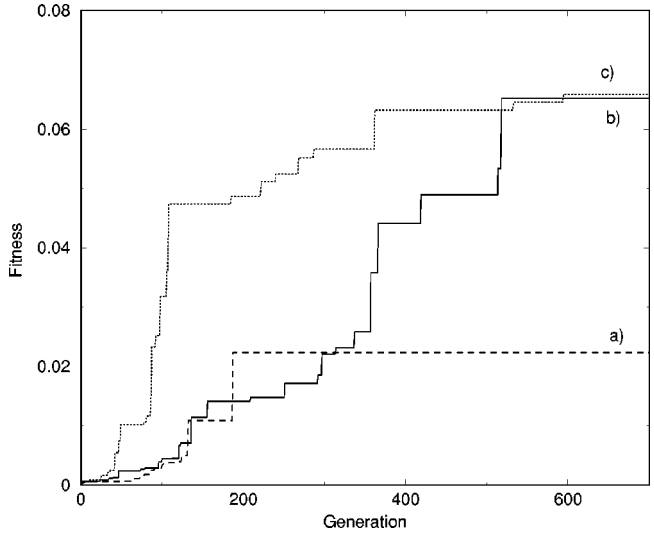

FIG. 2. Best fitness rule versus generation for three different runs. Lattice size is 10^3 cells. (a) Run in which rule ϕ_a was found at generation 188; (b) run in which rule ϕ_b was found at generation 518; (c) run in which rule ϕ_c was found at generation 594. The rules of the initial population were selected randomly with $0\leqslant\lambda\leqslant 1$ in runs (a) and (b), while in run (c) $0\leqslant\lambda\leqslant 0.5$.

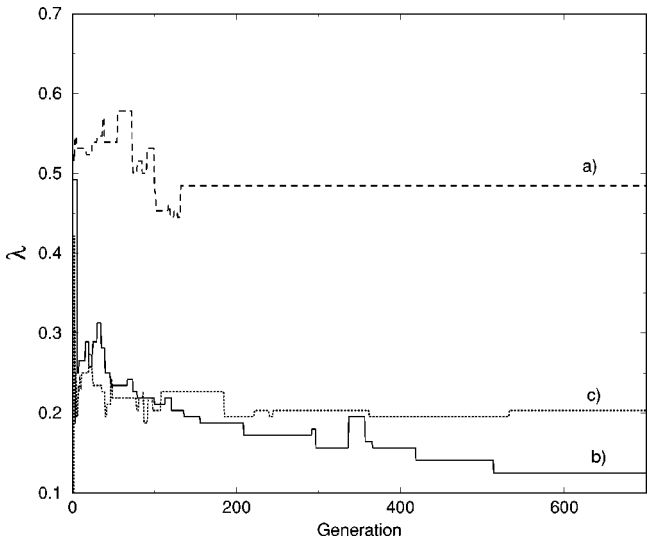

FIG. 3. Lambda parameter versus the generation for three different runs in which the following was detected. (a) rule ϕ_a; (b) rule ϕ_b, and (c) rule ϕ_c. As the GA evolves, λ of the best rules decreases.

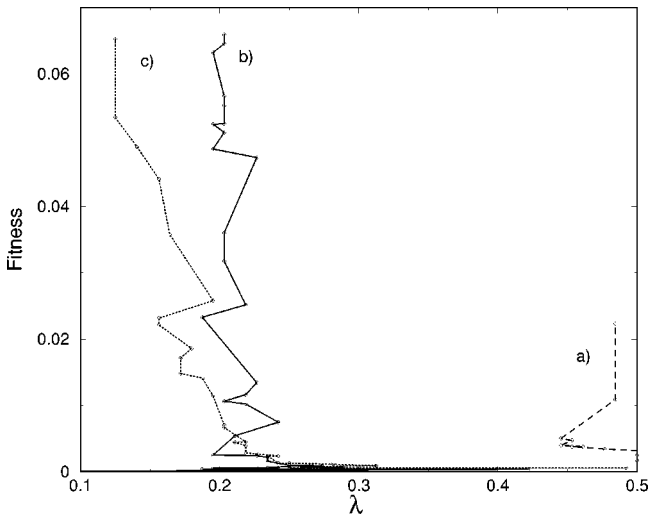

FIG. 4. Fitness function versus λ for runs (a), (b), and (c). Lattice size is 10^3 cells. Rules with high fitness values are found for $0.1<\lambda\leqslant 0.2$.

area of a noisy P1 and the area of an intermittent P2 are higher than that of a P2 and, finally, QP3 and P3 behaviors have the highest values.

In each generation, (i) $F(\phi)$ is calculated for each rule ϕ in the population; (ii) the population is ranked in order of fitness; (iii) a number E of the highest-fitness (''elite'') rules is copied without modification to the next generation; (iv) the remaining $P-E$ rules for the next generation are formed by single-point crossover between randomly chosen pairs of elite rules. The offspring from each crossover are each mutated with a probability m, where mutation consists of flipping a randomly chosen bit in a string. This defines one generation of the GA; it is repeated G times for one run of the GA.

V. RESULTS

We performed more than 50 different runs of the GA with the following parameters: $M=N/2=500$; $P=20$; $E=5$; $m=0.05$; $G=700$ (in some runs, G was set to 2000), each with a different random-number seed. The dynamics of three typical runs are shown in Fig. 2, which plots the fittest rule of each generation for three different runs (a), (b), and (c). Before the GA detects high-fitness rules, the fitness of the best CA rule increases by rapid jumps. Qualitatively, the rise in performance can be divided into several ''epochs,'' each corresponding to the discovery of a new, significantly improved strategy. The best evolved rule in each run is ϕ_a, which shows P4 behavior, ϕ_b (QP3) and ϕ_c (P3). In runs (a) and (b), the rules of the initial population had a random λ parameter in the range $[0,1]$, while in case (c) the selected λ was in the range $[0,0.5]$ (λ is defined as the fraction of nonzero output states in the rule table).

Figure 3 shows the λ parameter versus the generation for runs (a), (b), and (c). For each run it is observed that λ is decreasing as the GA is evolving. Table II shows the rule table in hexadecimal code, the type of nontrivial collective behavior, the fitness function, and the lambda parameter of the best evolved rules. Many of the CA rules that show P2 collective behavior map low values of concentration to high values and vice versa. These rules have a lookup table in which there is a balance between the regions of low and high concentration values and λ is around 0.5. Rules that show QP3 or P3 behavior, such as ϕ_b and ϕ_c, have a much lower value of λ. Figure 4 shows the fitness function versus λ for the three runs (a), (b), and (c). It has been suggested [9] that there is a relationship between the ability of a CA rule to show complex behavior and the λ parameter. The basic hypothesis was that λ correlates with computational capability in that rules capable of complex computation must be or are most likely to be found near some critical value λ_c. In our experiments we have found that rules with the highest values

TABLE II. Measured values of $F(\phi)$, the type of nontrivial collective behavior, and the λ parameter for different evolved rules: ϕ_a, ϕ_b, ϕ_c, and the rule-33 automaton. Lattice size is 10^3. To recover the 128-bit string giving the output bits of the rule table, expand each hexadecimal digit to binary. The output bits are then given in lexicographic order.

Symbol	Rule table hexadecimal code	NTCB	$F(\phi)$	λ
ϕ_a	b77f3839-bb50f61a-5773f461-0d104081	P4(P2)	0.022	0.484
ϕ_b	10000000-00080c22-00020c00-80864048	QP3	0.064	0.125
ϕ_c	1000008c-0008088c-0008808b-000d0bf1	P3	0.065	0.203
R_{33}	10000008-00080886-00080886-08868621	QP3	0.053	0.164

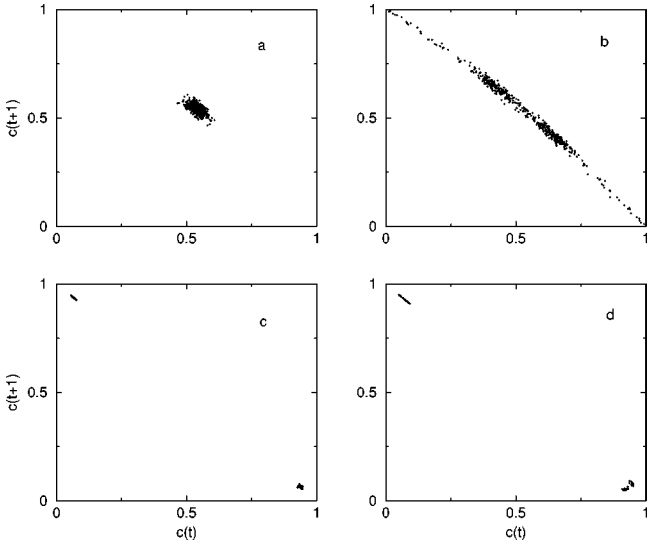

FIG. 5. Iterative map of the concentration of the fittest rule in the generation: (a) 55; (b) 63; (c) 132; (d) 188, the best rule ϕ_a. Lattice size is 10^3 cells.

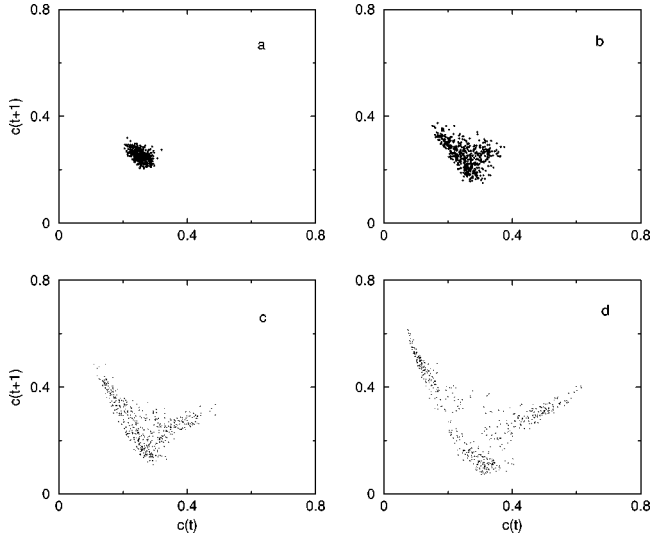

FIG. 7. Iterative map of the concentration of the fittest rule in the generation: (a) 8; (b) 100; (c) 156; (d) generation 518 (ϕ_b). Lattice size is 10^3 cells.

of F have a λ parameter in the range $0.1<\lambda\leqslant 0.2$.

Usually, the GA does not detect rules with QP3 or P3 behavior, but does detect rules with intermittent P2 or with P4 behavior such as the one shown in Fig. 2(a). The iterative map of the concentration for the fittest rule for different generations in run (a) is shown in Fig. 5. In the initial generations, the GA detects rules with noisy P1 behavior, and the concentration values are around 0.5. In generation 63 there is a jump in the fitness function as intermittent P2 behavior is found. Another important jump in $F(\phi)$ is observed at generation 132, when noisy P2 behavior is found. And finally, in generation 188, rule ϕ_a is detected. Rule ϕ_a shows P4 behavior, as can be seen clearly in Fig. 6. But in the iterative map—Fig. 5—three clouds of points can be seen: the P4 mimics P3 and this is why the GA selects rules like ϕ_a.

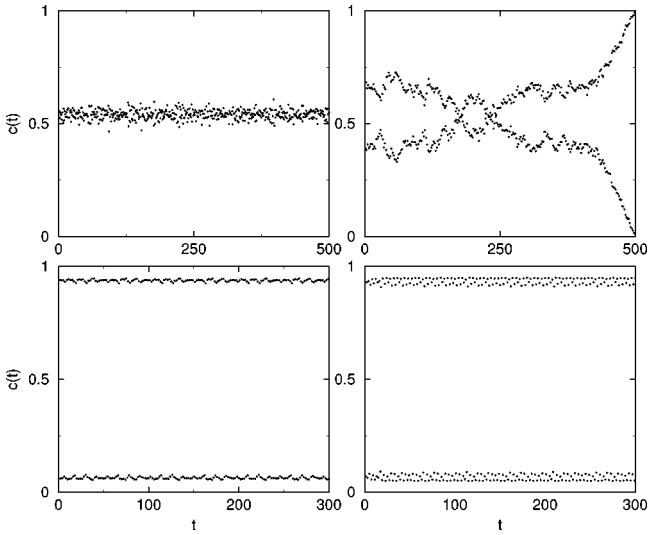

FIG. 6. Time series of the concentration corresponding to Fig. 5 for the fittest rule in the generation: (a) 55; (b) 63; (c) 132; (d) 188, the best rule ϕ_a. Lattice size is 10^3 cells.

When the lattice size increases, the P4 collective behavior changes to P2.

The iterative map of the concentration for the fittest rule for different generations in run (b) is shown in Fig. 7. In the initial generations, the GA detects rules with cloudy P1 behavior. In generation 100 the cloudy P1 widens and a triangular object can be seen. The GA has detected a new rule that improves the fitness significantly. Figures 7(c) and 7(d) correspond to the fittest rule in generations 156 and 518 (ϕ_b), where a QP3 can be seen clearly. In the case of QP3, as the lattice size increases the behavior is better defined.

To explain how the global coordination arises, it has been suggested in [10] that rules exhibiting quasiperiodic collective behavior are well described, at large scales, by the

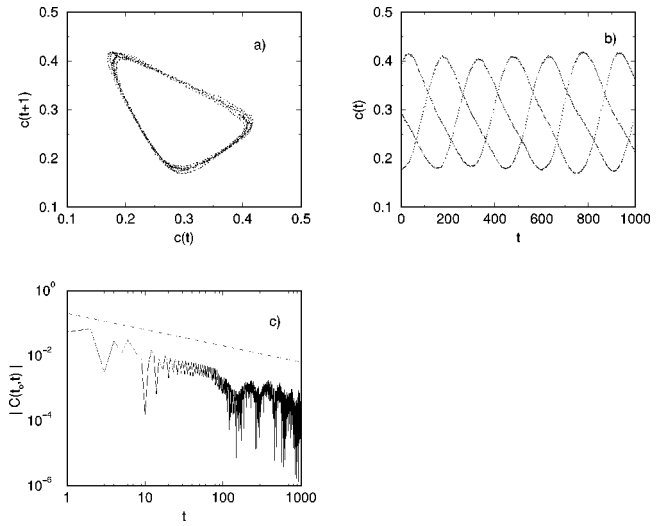

FIG. 8. QP3 collective behavior shown by rule ϕ_b, starting from a random initial concentration of 0.5. Lattice size is 10^6. Transient discarded. (a) The iterative map. (b) The time series of the concentration. (c) Log-log plot of the absolute value of the time autocorrelation function. The slope of the line is $-1/2$.

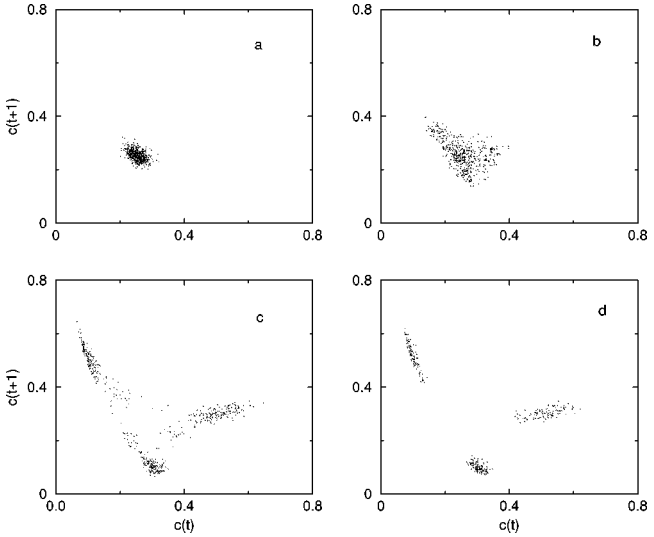

FIG. 9. Iterative map of the concentration of the fittest rule in the generation: (a) 10; (b) 49; (c) 98; (d) 594 (ϕ_c). Lattice size is 10^3 cells.

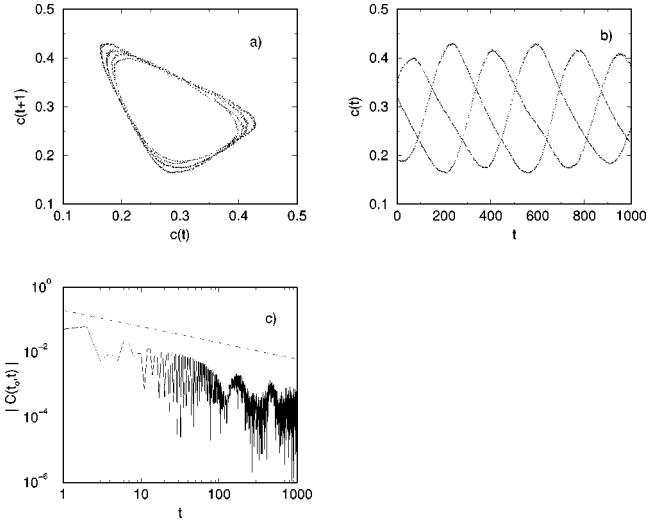

FIG. 10. QP3 collective behavior shown by rule ϕ_c, starting from a random initial concentration of 0.5. Lattice size is 10^6. Transient discarded. (a) The iterative map. (b) The time series of the concentration. (c) Log-log plot of the absolute value of the time autocorrelation function. The slope of the line is $-1/2$.

Kardar-Parisi-Zhang (KPZ) equation [11]. The local order parameter has a spatial average $<c_t(x)>=f(\omega t)$, where $f(\omega t)$ is a periodic function. Local variations can be incorporated by writing $c_t(x)=f[\omega t+\Phi_t(x)]$, where Φ is a fluctuating ''phase'' field. Then in a large system the coherence can only be maintained through the mutual coupling and entrainment of the local phases. One of the consequences of the KPZ equation for rules producing quasiperiod behavior is that the time autocorrelation function decreases asymptotically like $t^{-(d-2)/2}$.

Figure 8 shows the iterative map, the time series of the concentration, and the time autocorrelation of ϕ_b. The time autocorrelation function is defined as

$$C(t_o,t)=\frac{1}{n}\sum_{i,j,k}^{n}[s_{i,j,k}(t_o)s_{i,j,k}(t)-c(t_o)c(t)].$$

The absolute value of $C(t_o,t)$ on a log-log scale is shown in Figure 8(c). $C(t_o,t)$ oscillates in time and the envelope of the oscillation decays as a power law with an exponent ≈ 0.5, which is according to the prediction of the KPZ.

The best way for the GA to detect rules with QP3 or P3 collective behavior is to start out with an initial population of rules with $0 \leqslant \lambda \leqslant 0.5$, such as in run (c) of Fig. 2. The iterative map of the concentration for the fittest rule for different generations is shown in Fig. 9. Table III shows seven ancestors of the best evolved rule ϕ_c. In the initial generations the GA detect rules with cloudy P1 behavior as in the previous run (b) and with a small fitness $F(\phi_{10})=0.0006$. The rule table of ϕ_{10} reveals that the rule maps the all zeros neighborhood to 1. In generation 49 there is a big jump in $F(\phi_{49})=0.0101$, and in the iterative map a triangular object can be seen. Rule ϕ_{49} maps the all zeros neighborhood to 1 and neighborhoods with a small number of ones are mapped to 0. This seems to be one of the main characteristics of the best rules (see Table II).

Before generation 100, the GA has detected high-fitness rules with QP3 collective behavior $[F(\phi_{98})=0.0317]$. Rule ϕ_{98} maps more neighborhoods with low concentrations to 0 than rule ϕ_{49}. In generation 594 the GA detects a rule ϕ_c $[F(\phi_c)=0.066]$ that shows P3. Figure 10 shows the iterative map, the time series of the concentration, and the time autocorrelation of ϕ_c for a lattice size of 10^6 cells. When the

TABLE III. CA chromosomes (look-up table output bits) given in hexadecimal code, value of the fitness function and λ for seven ancestors of ϕ_c.

Generation	Rule table hexadecimal code	$F(\phi)$	λ
10	18004007-004a0868-82990002-420b6b60	0.0006	0.234
49	100008c6-004a0c0a-00088002-020b4be1	0.0101	0.219
98	1000008a-00080c0a-00088403-020b4be1	0.0317	0.203
200	10000088-0008080a-0008848b-000e0bf1	0.0487	0.195
300	10000086-0008080e-00088489-020a0bf1	0.0566	0.203
400	1000008c-00080888-0008808b-000d03f3	0.0632	0.195
550	1000008c-00080888-0008808b-000f0bf2	0.0645	0.203
594 (ϕ_c)	1000008c-0008088c-0008808b-000d0bf1	0.0659	0.203

FIG. 11. Space-time diagram of a layer-averaged concentration profile for rule ϕ_c starting from a random initial concentration. Transient discarded. Each dot represents an average over the concentration in a two-dimensional layer perpendicular to the x axis (white represents a concentration value for which $0 \leqslant c < 0.1$ and black for which $0.4 \leqslant c < 0.5$). Time goes downward and 200 time steps are shown. Lattice size is 10^6.

lattice size increases, the P3 collective behavior changes to QP3.

One successful approach to understanding the computation performed by evolved CAs is to adopt the computational mechanics framework developed by Crutchfield and Hanson for one-dimensional CAs. This framework describes the intrinsic computation embedded in the CA space-time configurations in terms of domains, particles, and particles interactions. Once a CA's regular domains have been detected nonlinear filters can be constructed to filter them out, leaving just the deviations from those regularities. The resulting filtered space-time diagram reveals the propagation of domain walls. If these walls remain spatially localized over time, they are called particles. Particles are one of the main mechanisms for carrying information over long space-time distances. In $d=2$ many difficulties arise when displaying the space-time diagram [12], and in $d=3$ the difficulties are greater because the space-time diagram is a four-dimensional surface. In order to grasp a picture of the space-time diagram, we take an approximation: the space is reduced to L cells of a given axis x, and the value of concentration in each point is an average over the concentration in a two-dimensional layer perpendicular to the x axis. Figure 11 shows a space-time diagram of a layer-averaged concentration profile of ϕ_c. Time goes downward and the value of the concentration sets the grayscale. Regular and synchronized regions that consist of alternating values of concentration, and some other irregular ones, can be observed. After the homogeneous regions have been filtered in Fig. 12, some propagating structures can be observed. However, a complete ''computational mechanics'' analysis of the evolved rules CAs is left for future work.

FIG. 12. Filtered space-time diagram corresponding to Fig. 11. Time goes downward (200 time steps are shown). Lattice size is 10^6.

VI. CONCLUSION

There is interest in developing scientific tools for understanding how spatially extended systems in nature perform computations. Using CA, two nontrivial problems—density and synchronization—have demonstrated that high performance systems can be developed to solve both. In this paper we have implemented a GA for a more complex task such as the appearance of nontrivial collective behavior. Under an appropriate fitness function, the GA selects preferentially rules with P3 and QP3 and the GA detects new CA rules in $d=3$ that show QP3 behavior. The evolutionary process can provide answers to the question of how nontrivial collective motion can be predicted. In our experiments as the GA is evolving λ parameter of the fittest rules is decreasing and the best rules are clustered in the range $0.1 < \lambda \leqslant 0.2$. We provide more numerical evidence that the time autocorrelation function of CA rules with QP3 decays with time as predicted by the Kardar-Parisi-Zhang equation and then the issue of how global coordination arises in the system can be addressed in terms of the entrainment of a local phase. Finally with the tools of the computational mechanics an averaged space-time diagram reveals propagating structures in the system.

ACKNOWLEDGMENTS

Many thanks are due to the EvCA group of SFI for their assistance and suggestions. This work was partially supported by Grant No. PB 97-0741 of the Spanish Government.

[1] M. Mitchell, J.P. Crutchfield, and P.T. Hraber, Physica D **75**, 361 (1994).
[2] J.P. Crutchfield and M. Mitchell, Proc. Natl. Acad. Sci. USA **92**, 10 742 (1995).
[3] R. Das, M. Mitchell, and J.P. Crutchfield, in *Parallel Problem Solving from Nature—PPSN III*, edited by Y. Davidor, H.-P. Schwefel, and R. Männer, *Lecture Notes in Computer Science, Volume 866* (Springer, Berlin, 1994), pp. 344–353.
[4] R. Das, J.P. Crutchfield, M. Mitchell, and J.E. Hanson, in *Proceedings of the Sixth International Conference on Genetic Algorithms*, edited by L.J. Eshelman (Morgan Kaufmann, San Francisco, 1995), pp. 336–343.
[5] C.H. Bennet, G. Grinstein, Yu. He. C. Jayaprakash, and D. Mukamel, Phys. Rev. A **41**, 1932 (1990).
[6] J. Hemmingsson, Physica A **183**, 225 (1992).
[7] H. Chaté and P. Manneville, Prog. Theor. Phys. **87**, 1 (1992).
[8] F. Jiménez-Morales and J.J. Luque, Phys. Lett. A **181**, 33 (1993).
[9] C.G. Langton, Physica D **42**, 12 (1990).
[10] H. Chaté, G. Grintein, and L. Tang, Phys. Rev. Lett. **74**, 912 (1995).
[11] M. Kardar, G. Parisi, and Y.C. Zhang, Phys. Rev. Lett. **56**, 889 (1986).
[12] F. Jiménez-Morales, J.P. Crutchfield, and M. Mitchell, in *Cellular Automata: Research Towards Industry*, edited by R. Serra, S. Bandini, and F. Suggi Liverani (Springer, London, 1998), pp. 3–14.